33rd Annual International Conference of the IEEE EMBS
Boston, Massachusetts USA, August 30 - September 3, 2011

# On sparse forward solutions in non-stationary domains for the EIT imaging problem

Panagiotis Kantartzis, and Panos Liatsis

*Abstract*— **In the forward EIT-problem numerical solutions of an elliptic partial differential equation are required. Given the arbitrary geometries encountered, the Finite Element Method (FEM) is, naturally, the method of choice. Nowadays, in EIT applications, there is an increasing demand for finer Finite Element mesh models. This in turn results to a soaring number of degrees of freedom and an excessive number of unknowns. As such, only piece-wise linear basis functions can practically be employed to maintain inexpensive computations. In addition, domain reduction and/or compression schemes are often sought to further counteract for the growing number of unknowns. In this paper, we replace the piece-wise linear with wavelet basis functions (coupled with the domain embedding method) to enable sparse approximations of the forward computations. Given that the forward solutions are repeatedly, if not extensively, utilised during the image reconstruction process, considerable computational savings can be recorded whilst maintaining $O(N)$ forward problem complexity. We verify with numerical results that, in practice, less than 5% of the involved coefficients are actually required for computations and, hence, needs to be stored. We finalise this work by addressing the impact to the inverse problem. It is worth underlining that the proposed scheme is independent of the actual family of wavelet basis functions of compact support.**

## I. INTRODUCTION

For the numerical solution of Partial Differential Equations (PDEs) on arbitrary domains the Finite Element Method (FEM) is the method of choice [3]. In particular, for relatively low-discretisation levels and, hence, coarse mesh models, the simplicity of FEM is hard to beat. As the discretisation fidelity is refined however, the resulting fine mesh model is characterised by an increasing number of degrees of freedom and excessive number of unknowns. Therefore, one resorts to implicit means of model reduction, as for instance the Boundary Element Method (BEM) [6] and/or adaptive refinement schemes [12].

Unfortunately, it is not always feasible to invoke a BEM solver as for instance in the case of PDEs of anisotropic coefficient distributions. In a similar manner, it is not always practical to apply adaptive refinement schemes since meshing the entire domain is a cumbersome and time-consuming procedure. Not to mention that meshing in non-stationary domains is a considerable task itself. This is the case for Electrical Impedance Tomography (EIT) where solutions on possibly non-stationary and anisotropic domains are sought.

In a typical EIT experimental setup, a prescribed current stimulation $\iota$ is applied to the boundary of the body and the developed fields $\upsilon$ are measured. The measured data set serves as the observable input to infer the unobservable (material) distribution. Remarkably, in EIT, a set of voltage measurements along with information about the underlined geometry properties, suffices to form an image of the interior material distribution. Indeed, EIT has been successful in reconstructing material distribution in a number of medical applications [1], [10], [15]. In general, EIT is considered as an inexpensive and portable modality capable of non-intrusively imaging the interior of a body.

In a typical clinical configuration, as for instance monitoring of lung activity [2], reconstructions need to take place in real-time. Moreover, since EIT is capable of operating on a 24/7 basis, vast data sets are anticipated, subject to (post-) processing and image enhancement algorithms. Taking into account the complexity of the chest area and the anisotropy of the human body, the FEM appears to be the method of choice. However, discretising such a 3D non-stationary domain can be a rather challenging step due to the aforementioned reasons. Indeed, for anisotropic problems the meshing procedure requires extra care to avoid undesirable and spurious effects during reconstructions.

In this paper, we propose the use of the Domain Embedding Method (DEM) coupled with uniform grids to confine the meshing procedure to the boundary surface in a spirit very similar to BEM. In view of sparsity and compression, we propose the use of B-Spline wavelet functions for the solution of the underlying Laplacian PDE. The suggested scheme enables asymptotically optimal preconditioning scheme as well as sparse approximations and, hence, in-house compression and adaptivity.

In the next section, we provide an overview of the image formation protocol in order to address how the proposed configuration affects the image formation process. Next, we give a quick overview of the carefully engineered weak (forward) formulation and discretisation. We finalise this study by providing the previously unavailable compression scheme for EIT along with concluding remarks on the impact to the inverse computations.

## II. THE FORWARD PROBLEM SETUP

The mathematical setup for the EIT problem is summarised by two problems; a forward and an inverse one. The former is the one of approximating the solution of a boundary value problem, given below in operator form as [7]

$$A_\sigma \upsilon = \iota \tag{1}$$

P. Kantartzis and P. Liatsis are with the Information Engineering and Medical Imaging Group, City University London, Northampton square, EC1V 0HB, London, UK. p.kantartzis@city.ac.uk

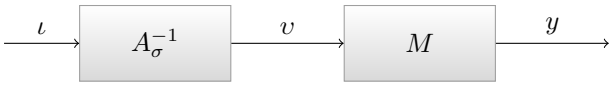


Fig. 1. The block diagram of the forward process. Currents are driven to the body and potentials are measured.

where $A_\sigma$ is the Laplacian operator (of a possibly anisotropic coefficient distribution $\sigma$, herein the material distribution) coupled with boundary conditions [14], $\upsilon := [u, U]^T$ the developed fields, $u$ is the interior potential distribution and $U := [U_1, \ldots, U_L]$ the surface potentials.

The latter problem is essentially an inverse boundary value problem, where one attempts to infer the unknown material distribution $\sigma$ based on surface measurements (potentials). In operator form the inverse (imaging) problem can be summarised by a non-linear forward operator $\Lambda$ as

$$\Lambda(\sigma) = y \tag{2}$$

The two problems (1) and (2) are linked using the measurement operator $M$ as

$$y = M\upsilon \tag{3}$$

which, typically, is a differential operator, i.e., transforming potential measurements $u|_{\partial\Omega}$ on the boundary $\partial\Omega$ to voltage measurements $y$.

### *A. Fast forward solutions are essential to the imaging process*

Note that in a typical optimisation scheme where $\sigma$ is estimated, the linearised version of the original problem (4) is obtained. Using first order approximation and by ignoring second order Taylor expansion terms one may obtain that

$$J_{\sigma_0}\delta\sigma = \delta y \tag{4}$$

where $J_{\sigma_0}$ is the Jacobian evaluated at $\sigma_0$, $\delta\sigma$:=$\sigma - \sigma_0$ and $\delta y := y - y_0$ is the difference in the measurement data set between two states of the material distribution $\delta\sigma$. This is often quoted as differential imaging.

For either linear or nonlinear iterative schemes, the efficient evaluation of the densely populated, ill-conditioned and rectangular matrix $J$ is of paramount importance. The adjoint fields method provides a means of numerically assembling this matrix in an efficient manner [13]. This method in turn necessitates the use of (repeated) solutions of the forward problem (1). Therefore, the forward problem (1) is fundamental to the actual imaging problem and is frequently quoted as the core EIT-imaging computation. The forward process, Equations (1) and (3), is illustrated in Figure 1 and summarised by Equation (2).

### *B. Standard weak formulation for EIT*

In this section the weak formulation for the EIT problem is derived for a bounded domain $\Omega \subset \Pi \subset \mathbb{R}^2$ in order to lay the foundation for the fundamental ideas presented in this paper. Assume that $L$ electrodes are attached on the Lipschitz boundary surface $\partial\Omega$ of $\Omega$. $\Gamma \subset \partial\Omega$ denotes the union of areas under each electrode, assumed to be open connected subsets

$$\bigcup_{l=1}^{L} \Gamma_l = \Gamma \tag{5}$$

and $\Theta := \partial\Omega \setminus \Gamma$ is the union of the remaining areas.

The so-called conductivity equation behind the EIT problem is a generalised Laplacian of the form

$$\nabla \cdot (\sigma \nabla u) = 0. \tag{6}$$

Boundary conditions on the electrodes $\Gamma$ are given below as

$$\sigma\nabla u \cdot \nu = \jmath \qquad \text{on } \Gamma, \tag{7}$$

$$u + z_l\sigma\nabla u \cdot \nu = U_l \qquad \text{on } \Gamma_l, \tag{8}$$

where $U_l, \nu, \imath, z_l$ the surface potential on the $l-$th electrode, the outward unit normal vector, the current density and the surface (electrode) impedance, respectively.

The boundary condition imposed on the interelectrode gaps is

$$\sigma\nabla u \cdot \nu = 0 \quad \text{on } \Theta. \tag{9}$$

Taking inner products of $L_2$ on both sides of the conductivity equation (6) and applying the vector identities along with the divergence theorem yields in

$$\int_\Omega \sigma\nabla v \cdot \nabla\overline{w}\, d\Omega = \int_{\partial\Omega} \sigma\nabla u \cdot \nu\overline{w} d\Gamma \tag{10}$$

and by substituting boundary conditions (8) and (9) in equation (10) one obtains

$$\int_\Omega \sigma\nabla u \cdot \nabla\overline{w}\, d\Omega = \sum_{l=1}^{L} \int_{\Gamma_l} \frac{1}{z_l} U_l\overline{w}\, d\Gamma_l - \sum_{l=1}^{L} \int_{\Gamma_l} \frac{1}{z_l} u\overline{w}\, d\Gamma_l. \tag{11}$$

Integrating (7) over the electrode area $\Gamma$ results to

$$\int_\Gamma \sigma\nabla u \cdot \nu\, d\Gamma = \int_\Gamma \jmath\, d\Gamma \tag{12}$$

or electrode-wise using (8)

$$\int_{\Gamma_l} \frac{1}{z_l} (U_l - u)\, d\Gamma_l = \Upsilon_l. \tag{13}$$

Following [14], the sesquilinear form is defined according to Equation (15) and the weak formulation of the EIT problem is stated as given the driving currents $\Upsilon = (\Upsilon_1, \ldots, \Upsilon_L)^T \in \mathbb{R}^L$, with $\Upsilon_l$ denoting the current applied to the $l$-th electrode, find $(u, U) \in \mathcal{H}^1_\Omega$ such that

$$a_\Omega((u, U), (v, V)) = \Upsilon^T\overline{V}, \text{ for all } (v, V) \in \mathcal{H}^1_\Omega \tag{14}$$

subject to uniqueness constraints $\sum_l U_l = 0$ and $\sum_l \Upsilon_l = 0$ [14]. The same authors define the quotient (uniqueness) solution space as $\mathcal{H}^1_\Omega := \mathcal{H}^1(\Omega) \oplus \mathbb{C}^L/\mathbb{C}$, where $(\mathcal{H}^1_\Omega)'$ denotes the dual Sobolev space [14].

$$a_\Omega((v,V),(w,W)) := \int_\Omega \sigma\nabla v\cdot\nabla\overline{w}\,d\Omega + \sum_{l=1}^{L}\int_{\Gamma_l}\frac{1}{z_l}(v-V_l)(\overline{w}-\overline{W}_l)\,d\Gamma_l. \tag{15}$$

$$a_\Pi((v,V),(w,W)) := \int_\Pi \sigma\nabla v\cdot\nabla\overline{w}\,d\Pi + \sum_{l=1}^{L}\int_{\Gamma_l}\frac{1}{z_l}(v-V_l)(\overline{w}-\overline{W}_l)\,d\Gamma_l. \tag{16}$$

$$\inf_{(v,V)\in\mathcal{H}^1_\Pi}\sup_{q\in\left(\mathcal{H}^{1/2}(\Theta)\right)'}\left\{\frac{1}{2}a_\Pi((v,V),(v,V)) - \Upsilon^T\overline{V} + b(v,q)\right\} \tag{17}$$

## III. Extending the original domain to a fictitious domain

Central to this contribution is the following, non-typical, intermediate-step. In particular, we assume that the original domain is extended to a slightly larger arbitrary one denoted as $\Pi$. This is the so called DEM-paradigm, originally derived to accommodate the anticipated deformations of the evolving boundary surface [11], [7]. Taking suitable extensions for all functions from $\Omega$ to the fictitious domain $\Pi$, the sesquilinear form in $\Pi$, denoted as $a_\Pi(\cdot,\cdot)$, is defined according to Equation (16).

Unfortunately, (15) and (16) are not equivalent [7], [9]. This is due to the fact that in the interelectrode gaps ($\Theta$), the current flux (9) in the original domain $\Omega$ is implicitly encapsulated in $a_\Omega$ (but vanishes). The same condition is not fulfilled by $a_\Pi$. In other words, there is no restriction about the flux of the potentials in the new fictitious domain $\Pi$. Therefore, the solution space needs to be constrained using (9).

### A. Lagrangian constraints

We opt for the Lagrange multiplier technique to enforce the essential boundary condition to the fictitious domain $\Pi$ by setting the appropriate functional, shown in Equation (17), where

$$b(v,q) := \int_\Theta q\sigma\nabla v\cdot\nu\,ds. \tag{18}$$

The standard first order optimality conditions then read

$$a_\Pi((u,U),(v,V)) + b(v,p) = \Upsilon^T\overline{V} \tag{19}$$

$$b(u,q) = 0. \tag{20}$$

for an excitation pattern $\iota$, defined as $\iota := [\Upsilon^T\overline{V},0]^T$. For a discussion on existence and uniqueness of the proposed scheme as well as the definition of the involved spaces, we refer to [7].

### B. Bypassing the domain discretisation burden

In order to simplify the domain discretisation in the new fictitious domain $\Pi$, one opts for a (numerically) convenient to discretise shape. In this paper, we opt for a square domain. The rationale is two-fold. Recasting the forward EIT problem under the square domain enables us to avoid expensive (re-) meshing algorithms for domain computations. In practice, only boundary surface meshing is required as in the BEM. Recall however, that the obtained stiffness matrices in BEM are indefinite, densely populated and for the EIT case non-square ones typically resorting in Least-Square type of solutions. It is worth underlining that this is not the case with the present formulation; involved matrices are both square and sparse.

On the other hand, one may opt for a uniform grid discretisation on the new square domain similarly to the Finite Difference Method (FDM). Note that the FDM is limited to very simple rectangular domains, far from the ones encountered in EIT. However, for our purposes the square domain encapsulates the original arbitrary one, whilst simplifying numerical treatment.

## IV. Discretisation

Having derived the DEM formulation to both allow deformations as well as to eliminate the need for meshing the domain, we now proceed with the discretisation of the continuous problem based on linear B-Splines basis functions of compact support.

Assuming a finite subspace $S_j \subset L_2$ spanned by dilated translates of the basic spline $\varphi$, with respect to a uniform grid spacing $h = 2^{-j}$, the functions involved in the EIT formulation are assumed to be linear combinations of B-spline functions

$$u(\mathbf{x}) = \sum_{\mathbf{k}}\mathbf{c_k}\varphi\left(\frac{\mathbf{x}}{2^j}-\mathbf{k}\right) \tag{21}$$

$$v(\mathbf{x}) = \varphi\left(\frac{\mathbf{x}}{2^j}-\mathbf{k}'\right). \tag{22}$$

It is worth stressing that having Splines on board suits best the uniform grid discretisation concept for $\Pi$. Additional advantages in our proposed coupling with B-splines is that (as in FDM) domain integrals and correspondingly associated derivatives have fixed, non-zero entries, which can be precalculated and serve as a lookup table. This enables a banded structure for the stiffness matrix as opposed to scattered matrix entries in typical FEM-based matrices. We underline that all the above remarks are independent of the linear B-spline chosen herein and hold valid for B-splines of higher orders if desired.

In view of the ultimate goal of this configuration, i.e., sparsity of the forward solutions, we can push the analysis a step further since B-Splines admit multiresolution. In fact, the main contribution of this paper is to combine DEM with B-Spline wavelets. Using the so-called wavelet transform and thanks to the carefully engineered formulation, one may

conveniently switch discretisation from B-Splines to wavelet basis functions as

$$T^T A_\sigma T T^{-1} u = T^T \iota \tag{23}$$

where $T$ is the so called wavelet transform. The wavelets considered herein are biorthogonal (Riesz) basis functions. In particular, we employ tensor products of the biorthogonal Spline-wavelets from [4], adapted to the interval as in [5].

Crucially for the analysis described in this paper, the proposed configuration based on wavelets results to a multilevel solution $T^{-1}u$, where wavelet coefficients $\mathbf{d_k}$ are retrieved instead instead of spline coefficients $\mathbf{c_k}$, see Equation (21). Given that the wavelet transform is a 'sparsity transformation', the obtain solution, i.e., wavelet coefficients $\mathbf{d_k}$, will maintain a sowewhat sparse structure. Further details concerning the wavelet transform for the EIT case are provided in [7].

*1) Domain Discretisation:* For functions defined on the domain $\Pi$, discretisation can be performed in a rather trivial way thanks to the square (fictitious) domain, allowing for uniform grid discretisation (of pitch $h$). In order to demonstrate the advantages of the suggested concept, we register to the fictitious domain $\Pi$ a *circular* domain $\Omega$ of radius 1/4, centered at (1/2,1/2), with 8 electrodes attached holding fixed contact impedance values set to $z = 10\,\Omega$hm (see Fig. 2).

*2) Boundary Discretisation:* The discretisation of the boundary contour itself is a delicate issue. Following the dyadic discretisation of the $\Pi$ domain, we opt for a dyadic discretisation for $\partial\Omega$ by splitting the boundary curve into an equivalent (dyadic) number of nodes. Note that functions on the boundary require different discretisation levels due to the so called LBB condition [8], [9].

## V. Numerical Results

In this section, a numerical experiment is set to demonstrate the ideas developed in this paper. Current is applied between electrodes 1 & 6 and the multilevel potential distribution (wavelet coefficients $\mathbf{d_k}$) in the interior is illustrated in Fig. 3 where at each decomposition level the original domain is superimposed to the fictitious one.

The DEM appears to increase the size of the solution space as the original domain needs to be prolonged to a square. A careful observation of the distribution of the coefficients (Fig. 4, top) however reveals that most of the coefficients are almost zero (Fig. 4, bottom). By discarding coefficients with absolute values of less than the typical instrumentation/mesurement noise, say $10^{-6}$, it turns out that the ratio of the non-zero over the total ones is $4.8\%$. This indicates that, roughly, only $5\%$ of the total number of coefficients is essentially required. Indeed, this demonstrates the superior advantage of the suggested scheme against the conventional ones. One may discard coefficients in low absolute values and store the essential ones. In this case, only a few. This suggests an efficient yet implicit compression scheme and paves the way for adaptive wavelet schemes.

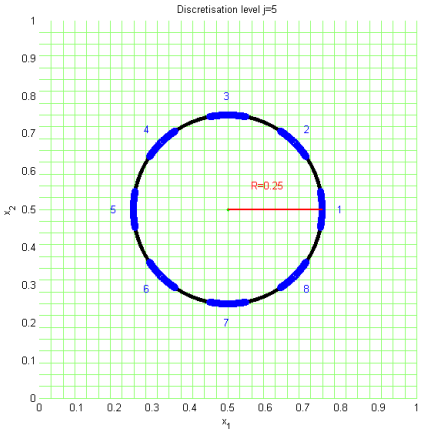


Fig. 2. The original circular geometry $\Omega$ is superimposed to the fictitious domain $\Pi$. 8 electrodes are attached (blue arcs) to the surface of the original domain.

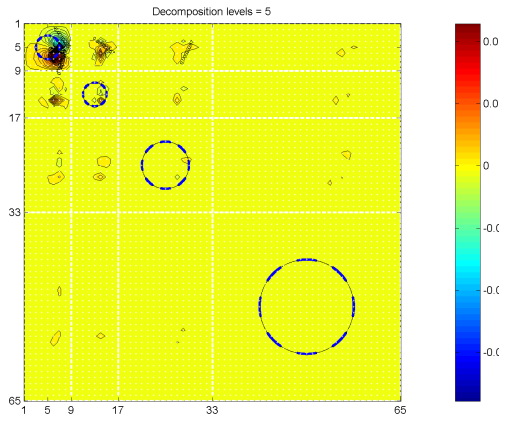


Fig. 3. The multilevel and sparse structure of the forward solution when current is applied between electrodes 1 and 6.

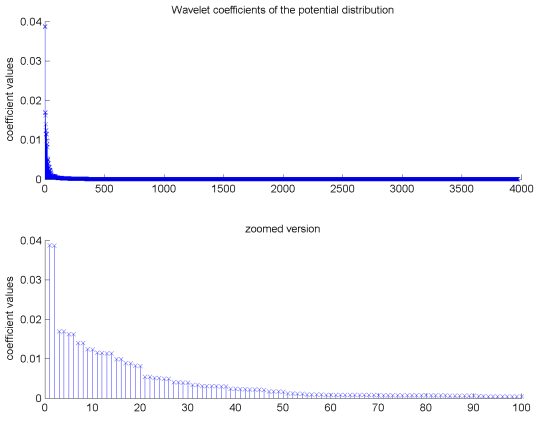


Fig. 4. Absolute values of wavelet coefficients. Top: The wavelet coefficient distribution. Bottom: Zoomed-in version.

## VI. Discussion

It is worth underlying that aside from compression, the suggested framework is known to result in optimal $O(N)$ operations by means of an asymptotically optimal preconditioning scheme for EIT [8], where $N$ in the number of unknowns. Further, mesh discretisation is practically limited to the circumference of the circle, i.e., line discretisation instead of domain discretisation. Indeed, taking into account the sparse structure of the solution, the suggested scheme can be considered as an 'implicit model reduction scheme'.

On the other hand, since such properties can be carried forward to the rest of the analysis for the inverse problem, Equation (2) or (4), the actual impact of this configuration to reconstructions can be tremendous. This will allow us to directly infer distributions in a sparse structure, acknowledging even further computational and storage savings. Indeed, a sparse-multilevel forward configuration may additionally enable hierarchical reconstruction algorithms, i.e., taking full advantage of the proposed multilevel structure.

## VII. Conclusions

In this paper, the standard weak formulation of EIT was considered and a continuous-space extension to DEM was proposed. The theoretical equivalence between original and fictitious domain was addressed and discretisation was performed in terms of B-Spline Wavelets. The proposed scheme resulted in sparse forward solutions where only a few coefficients are zero. The suggested multilevel configuration is not limited to the forward problem. Indeed, it carries forward to the inverse problem in order to enable inherently sparse reconstructions. Finally, it is worth highlighting that the suggested formulation can be trivially extended to 3D by means of tensor products of the associated basis functions.

## VIII. ACKNOWLEDGMENTS

We gratefully acknowledge financial support by the Engineering and Physical Sciences Research Council (EPSRC) under Grant EP/G061580/1 and the State Scholarships Foundation of Greece (IKY). We would also like to thank the anonymous reviewers for their valuable comments.

## References

[1] A. Adler, R. Guardo, and Y. Berthiaume, "Imaging of gastric emptying with electrical impedance tomography," *Canadian Medical and Biolological Eng. Soc.*, vol. 20, Vancouver, Canada 1994.

[2] A. Adler, J. H. Arnold, R. Bayford, A. Borsic, B. Brown, P. Dixon, T. J. C. Faes, I. Frerichs, H. Gagnon, Y. Grber, B. Grychtol, G. Hahn, W. R. B. Lionheart, A. Malik, R. P. Patterson, J. Stocks, A. Tizzard, N. Weiler, and G. K. Wolf, "GREIT: a unified approach to 2d linear eit reconstruction of lung images," *Physiological Measurement*, vol. 30, no. 6, p. S35.

[3] F. Brezzi and M. Fortin, *Mixed and Hybrid Finite Element Methods*. New York: Springer, 1991, vol. 15.

[4] A. Cohen, I. Daubechies, and J. C. Feauveau, "Biorthogonal bases of compactly suppoerted wavelets," *Comm. Appl. Math.*, vol. 45, pp. 485–560, 1992.

[5] W. Dahmen, A. Kunoth, and K. Urban, "Biorthogonal spline-wavelets on the interval — stability and moment conditions," *Appl. Comp. Harm. Anal.*, vol. 6, pp. 132–196, 1999.

[6] R. Duraiswami, G. L. Chahine, and K. Sarkar, "Boundary element techniques for efficient 2-d and 3-d electrical impedance tomography," *Ch. Eng. Sc.*, vol. 52, no. 13, pp. 2185 – 2196, 1997.

[7] P. Kantartzis, "Multilevel soft-field tomography," Ph.D. dissertation, City University London, 2010, (submitted).

[8] P. Kantartzis, A. Kunoth, A. Pabel, and P. Liatsis, "Wavelet preconditioning for eit," *J. Phys: Conf. Ser.*, vol. 224, no. 1, p. 012023, 2010.

[9] P. Kantartzis, A. Kunoth, R. Pabel, and P. Liatsis, "Towards non-invasive eit imaging of domains with deformable boundaries," *IEEE EMBC*, pp. 4991–4995, 2010.

[10] T. J. Kao, D. Isaacson, J. C. Newell, and G. J. Saulnier, "A 3D reconstruction algorithm for EIT using a handheld probe for breast cancer detection," *Phys. Meas*, vol. 27, no. 5, pp. S1–S12, 2006.

[11] A. Kunoth, *Wavelet Methods — Elliptic Boundary Value Problems and Control Problems*. B.G. Teubner, 2001.

[12] M. Molinari, "High fidelity imaging in electrical impedance tomography," Ph.D. dissertation, University of Southampton, 2003.

[13] N. Polydorides and W. R. B. Lionheart, "Adjoint formulations in impedance imaging," *Proc. 3rd Cong. Indust. Proc. Tomog.*, 2003.

[14] E. Somersalo, M. Cheney, and D. Isaacson, "Existence and uniqueness for electrode models for electric-currentcomputed tomography," *SIAM J. App. Math.*, vol. 52, no. 4, pp. 1023–1040, 1992.

[15] C. Soulsby, E. Yazaki, and D. F. Evans, "Applications of electrical impedance tomography in the gastrointestinal tract," *Electrical Impedance Tomography: Methods, History and Applications, Ed. D. S. Holder, Institute of Physics Publishing*, pp. 191–207, 2005.